Consequences of Lipid Droplet Coat Protein Downregulation in Liver Cells

Abnormal Lipid Droplet Metabolism and Induction of Insulin Resistance

Ming Bell,[1] Hong Wang,[1] Hui Chen,[2] John C. McLenithan,[3] Da-Wei Gong,[3] Rong-Zee Yang,[3] Daozhan Yu,[3] Susan K. Fried,[3] Michael J. Quon,[2] Constantine Londos,[4] and Carole Sztalryd[1]

OBJECTIVE—Accumulation of intracellular lipid droplets (LDs) in non-adipose tissues is recognized as a strong prognostic factor for the development of insulin resistance in obesity. LDs are coated with perilipin, adipose differentiation–related protein, tail interacting protein of 47 kd (PAT) proteins that are thought to regulate LD turnover by modulating lipolysis. Our hypothesis is that PAT proteins modulate LD metabolism and therefore insulin resistance.

RESEARCH DESIGN AND METHODS—We used a cell culture model (murine AML12 loaded with oleic acid) and small interfering RNA to directly assess the impact of PAT proteins on LD accumulation, lipid metabolism, and insulin action. PAT proteins associated with excess fat deposited in livers of diet-induced obese (DIO) mice were also measured.

RESULTS—Cells lacking PAT proteins exhibited a dramatic increase in LD size and a decrease in LD number. Further, the lipolytic rate increased by ~2- to 2.5-fold in association with increased adipose triglyceride lipase (ATGL) at the LD surface. Downregulation of PAT proteins also produced insulin resistance, as indicated by decreased insulin stimulation of Akt phosphorylation ($P < 0.001$). Phosphoinositide-dependent kinase-1 and phosphoinositide 3-kinase decreased, and insulin receptor substrate-1 307 phosphorylation increased. Increased lipids in DIO mice livers were accompanied by changes in PAT composition but also increased ATGL, suggesting a relative PAT deficiency.

CONCLUSIONS—These data establish an important role for PAT proteins as surfactant at the LD surface, packaging lipids in smaller units and restricting access of lipases and thus preventing insulin resistance. We suggest that a deficiency of PAT proteins relative to the quantity of ectopic fat could contribute to cellular dysfunction in obesity and type 2 diabetes. ***Diabetes*** **57:2037–2045, 2008**

From the [1]Geriatric Research, Education and Clinical Center, Baltimore Veterans Affairs Health Care Center, Division of Gerontology, Department of Medicine, School of Medicine, University of Maryland, Baltimore, Maryland; the [2]Diabetes Unit, National Center for Complementary and Alternative Medicine, National Institutes of Health, Bethesda, Maryland; the [3]Division of Endocrinology, Department of Medicine, School of Medicine, University of Maryland, Baltimore, Maryland; and the [4]Laboratory of Cellular and Developmental Biology, National Institute of Diabetes and Digestive and Kidney Diseases, National Institutes of Health, Bethesda, Maryland.

Corresponding author: Carole Sztalryd, csztalry@grecc.umaryland.edu.

Received 8 February 2008 and accepted 7 May 2008.

Published ahead of print at http://diabetes.diabetesjournals.org on 16 May 2008. DOI: 10.2337/db07-1383.

The surge in obesity predicts a further increase in associated complications, insulin resistance, diabetes, and heart disease (1,2). Increased fatty acid availability in obesity is associated with accumulation of ectopic fat, mainly in the form of triacylglyerol (TAG) (3). Although ectopic fat correlates with systemic and tissue insulin resistance (4–6), a number of circumstances are known in which high tissue lipid stores are not associated with insulin resistance. Endurance-trained athletes have high intramyocellular lipids yet are highly insulin sensitive. Importantly, the size and intracellular distribution of lipid droplets (LDs) differs in muscle from insulin-sensitive athletes compared with insulin-resistant patients (7). Thus, the negative consequences of high cellular lipids may be related to the ability of the cell to regulate lipid storage and utilization.

LDs are energy-storage organelles but have a surprisingly complex function in lipid homeostasis. LD biogenesis is a fundamental cellular function; when exposed to nonesterified fatty acids (NEFAs), cells store them as TAG in LDs (8). Such LD accumulation maintains low intracellular NEFAs, avoiding their toxic effects on cellular physiology while supporting cellular needs by releasing NEFAs for use in β-oxidation and membrane synthesis. LDs' function to sequester and release NEFAs is thus critical for proper cellular function. Nonadipogenic tissues in patients with metabolic syndrome are exposed to chronically elevated serum levels of NEFAs, and these tissues respond by LD accumulation. Such ectopic fat deposition protects from NEFA-mediated lipotoxicity (9), but in patients with metabolic syndrome the LD is inadequate to prevent pathological consequences. An important question arises: what molecular mechanisms regulate lipid storage in nonadipogenic tissues?

To date, we have only limited information on nonadipose LDs. Recent studies (10,11) identified a proteomic "signature," consistently including at least one member of the PAT protein family: perilipin, adipose differentiation–related protein (ADFP), tail interacting protein of 47 kDa (Tip47), S3–12, and lipid dosage droplet protein-5 (LSDP-5). Despite tissue dependence, the ubiquitous nature of the family suggests an important role in LD machinery. ADFP, Tip47, and LSDP-5 are broadly distributed, notably in nonadipogenic liver and muscle tissues that do not express perilipin (13,24). Our hypothesis is that saturation of nonadipogenic tissue's capacity to appropriately regulate storage and release of NEFAs via LDs results from varia-

tions in the expression and/or activity of PAT proteins. To study functional consequences of downregulating two major PAT proteins, ADFP and Tip47, on insulin resistance and lipid metabolism, we used small interfering RNA (siRNA) in a cell culture model. To assess the in vivo relevance of this finding, we measured the expression of PAT proteins associated with excess lipids accumulated in the livers of high-fat–fed obese mice.

RESEARCH DESIGN AND METHODS

Cell culture. AML12 cells (Dr. Steven Farmer, Boston University, Boston, MA) were grown with the standard protocol (American Type Culture Collection, Manassas, VA). For siRNA experiments, cells were plated in 24 multiwell dishes (Costar; Thermo Fisher Scientific, Pittsburgh, PA) at a density of 1×10^4 cells per well, transfected the next day with Hyperfect (Qiagen, Valencia, CA) according to the manufacturer's instructions. For immunocytochemistry, cells were plated in four-well chamber slides (Labtek; Thermo Fisher Scientific). For insulin-signaling assays, cells were deprived of insulin for 24 h and for the last 12 h were incubated in Dulbecco's modified Eagle's medium (DMEM)/F-12 media (1:1) containing 1% defatted BSA (Sigma-Aldrich, St. Louis, MO) and supplemented with 400 μmol/l oleic acid complexed to 0.4% BSA to promote TAG deposition. The next day, cells were incubated in DMEM/F-12 media (1:1) containing 1% defatted BSA (Sigma-Aldrich) for 6 h before a 10-min incubation with insulin at the concentration indicated. Cells were harvested in cold lysis buffer (150 mmol/l NaCl; 50 mmol/l Tris-HCl, pH 7.5; 1% Triton X-100; 0.5% NP-40; 0.25% sodium deoxycholate; 1 mmol/l EDTA; 1 mmol/l EGTA; 0.2 mmol/l ortho-vanadate; 1 mmol/l NaF; and protease inhibitor cocktail) (Roche Applied Science, Indianapolis, IN).

Oligos. siRNA was purchased from Qiagen (HP-guaranteed siRNA). Positive siRNA for map kinase 1 and fluorescent oligos (Qiagen) were used to establish efficient conditions for transfection to obtain 80% inhibition by Western blot (12) versus All Star negative control. For off-target toxicity, we used siRNA negative for insulin signaling: a negative siRNA targeting ADFP with a two-base mismatch (Ctl1), sense sequence 5′AACGTCTGCT**TGAG**CCGAATA-3′ (online appendix Fig. S-9 [available at http://dx.doi.org/10.2337/db07-1383]); and a negative −siRNA targeting Tip47 (Ctl2), sense sequence 5′-GCGUGUCCAAUCAGUCAU-3′ (12). Sense sequences for Tip47 (5′-AACAGCACAGAGAAUGAGGAG-3′) and ADFP (5′-AACGTCTGTCTGGACCGAATA-3′) were selected by potency. Total siRNA per well was 10 nmol/l for all transfections; for double transfection using one-third Tip47 and two-thirds ADFP siRNA; for triple using one-fourth Tip47, one-half ADFP, and one-fourth adipose triglyceride lipase (ATGL) siRNA; and downregulation confirmed (online appendix Figs. S-4 and -7). siRNA for ATGL was reported (35) and confirmed by imunoblot (Fig. S-3). siRNA efficiencies were quantified by Western blot (Un-scan; Silk Scientific, Orem, UT) and results expressed as percentage of control.

Liver tissues from DIO and ad libitum mice. C57BL/6 (8 weeks old) mice were ad libitum fed either a high-fat (60% kcal fat; Research Diets, New Brunswick, NJ) diet containing primarily lard or a low-fat (10% kcal fat, Research Diets) diet for 12 weeks. Mice on the high-fat diet exhibited diet-induced obesity (1.52-fold increase in body weight over low-fat–fed control mice) and impaired glucose tolerance (data not shown). On the day of the experiments, animals were killed by cervical dislocation and tissues were immediately frozen in liquid nitrogen. Tissue lipid was extracted (40) and expressed as percent lipid weight divided by total sample weight (mg/mg).

Antibodies and dyes. Rabbit anti-Tip47, LSDP-5, and goat anti-ADFP were used (12,13). Neutral lipid dye bodipy 558/568, alexa fluor 488, hoescht, and alexa fluor 598 species-specific secondary antibodies were from Molecular Probes (Invitrogen, Carlsbad, CA). Rabbit antibodies against human ATGL (Rockland Immunochemicals for Research, Gilbertsville, PA) were tested in human preadipocytes and 3T3-L1 adipocytes and in human and mice adipose tissues (M.B., C.S., and Mee Jeong Lee, unpublished data) or purchased, as were Akt, phosph-Akt, PDK-1, GS3-Kα, phosphor–GS3-K α, phospho-specific antibodies to protein kinase C (PKC), extracellular signal–regulated kinase (ERK), ERK-phosp antibodies (Cell Signaling technology, Beverly, MA), phosphor–insulin receptor substrate (IRS)-1 (Ser307) (Upstate Biotechnology, Lake Placid, NY), IRS-1 and Foxo-1 (Santa Cruz Biotechnology, Santa Cruz, CA), and β-actin (Abcam, Cambridge, U.K.). CGI-58 was a gift (Dr. Brasaemle, Rutgers University, Newark NJ) (31). Phospho-specific antibodies to PDK-1 were a gift from Dr. Quon. Immunoprecipitation for IRS-1 was performed as described (36).

Immunocytochemistry and immunoblotting. Fixation and staining were performed as described (12). Cells were viewed with a confocal laser microscope using a ×63 or ×40 oil objective lens. LD size was determined (LSM510; Carl Zeiss MicroImaging). Cellular extracts for immunoblot were obtained by scraping cells in Laemmli sample buffer. Each SDS-PAGE lane was loaded with protein from a single well of a 24-multiwell dish. Four wells were pooled for each data point for insulin signaling immunoblots. Quantitative analysis was performed using Un-scan (Silk Scientific Corporation). ^{32}PI3P (phosphatidylinositol 3 phosphate) bands were revealed by PhosphorImager (Storm 860; GE Healthcare) and band intensities quantified (ImageQuant 5.0; GE Healthcare). Live cell imaging was performed using an axiovert 200 microscope equipped with a camera (Carl Zeiss).

Cellular triglyceride turnover. Triglyceride synthesis and lipolysis were performed (21,39). Briefly, cells were incubated for 12 h with growth medium supplemented with 400 μmol/l oleic acid complexed to 0.4% BSA to promote triacylglycerol deposition. [^{3}H]oleic acid, at 1×10^6 dpm/well, was included as a tracer. In lipolysis experiments, reesterification of fatty acids in AML12 cells was prevented by inclusion of 10 μmol/l triacsin C (Biomol, Plymouth Meeting, PA), an inhibitor of acylcoenzyme A synthetase, in the medium (21,38,39). Quadruplicate wells were tested for each condition. Lipolysis was determined by measuring radioactivity release (12,21,39).

Lipid extraction and thin-layer chromatography. Cell monolayer was washed with ice-cold PBS and scraped into 1 ml PBS. For total TAG, lipids were extracted by the Dole method (40) from five wells of a 24-mutiwell dish. The total upper phase was dried down, resuspended in isopropanol, and assayed with a triglyceride kit (Wako Chemicals, Richmond, VA). Protein was measured by a kit (Pierce Biotechnology, Rockford, IL). For triglyceride synthesis, lipids were extracted by the Bligh-Dyer method (41) and 10% of the total lipids were analyzed with thin-layer chromatography extractions performed as reported (37,38) (see online appendix). Intracellular diacylglycerol, NEFAs, and ceramide were measured by analytical service (Avanti Polar Lipids, Albaster, AL) (43).

Glucose output. Measurements were performed according to Berusi et al. (48). Briefly, 2 days following siRNA transfection, cells were incubated in DMEM/F12 medium containing 1% BSA, 1 μmol/l dexamethasone (Sigma-Aldrich), and 1 μmol/l cAMP (EMD Chemicals, Gibbstown, NJ) for 24 h. Cells were incubated in 0.35 ml (per well) of phenol red–free, glucose-free DMEM containing 2 mmol/l pyruvate and 20 mmol/l lactate containing dexamethasone and cAMP. Some wells also contained insulin (10^{-8} mol/l concentration). Media was collected 5 h later for glucose measurement (48) with a fluorimeter (Molecular Devices, Union City, CA) in triplicate. Glucose output rate was normalized by cellular protein concentration and expressed as nanomols of glucose per milligram of protein every 5 h. Two separate experiments were performed.

Fat cake preparation. Four 24-mutiwell dishes for each condition were treated with siRNA negative or ADFP and Tip47. LD isolation was as reported (25). Total homogenate protein was determined and adjusted to 1 μg/μl. The lipid fat cake was isolated and suspended in 200 μl PBS containing 5% SDS.

Statistical analysis. Statistical significance was by one-way ANOVA or two-tailed Student's t test. (GraphPad software, San Diego, CA).

RESULTS

AML12 cell LDs contain mostly ADFP at the surface. After incubation of AML12 liver cells with 400 μmol/l oleic acid, numerous LDs appear, and most are coated with ADFP and fewer with Tip47 (Fig. 1*A*). Relatively few exhibit colocalized ADFP and Tip47 at the surface. ADFP was found exclusively at LD surfaces, while Tip47 was found in both cytosolic and LD compartments. Other PAT proteins were not detected by imunocytochemistry or immunoblot (results not shown). Hence, AML12 cells express two PAT proteins, ADFP and Tip47.

PAT protein downregulation induces change in LD morphology and surface profile. The effect from downregulation of Tip47, ADFP, or both with siRNA are shown in Fig. 1*B* and *C*. siRNA transfection produced minimal cellular toxicity from unchanged levels of β-actin. Efficiency of Tip47 inhibition was >95%, and efficiency of ADFP inhibition was 80%. siRNA treatments effectively produced droplets coated with only one of two PAT proteins or none (Fig. 1*B*). ADFP downregulation led to a dramatic increase in Tip47 protein at the LD surface, although total Tip47 protein in homogenates was not affected by increased exogenous oleic acid (online appendix Fig. S-1). Thus, increased Tip47 at the LD surface is

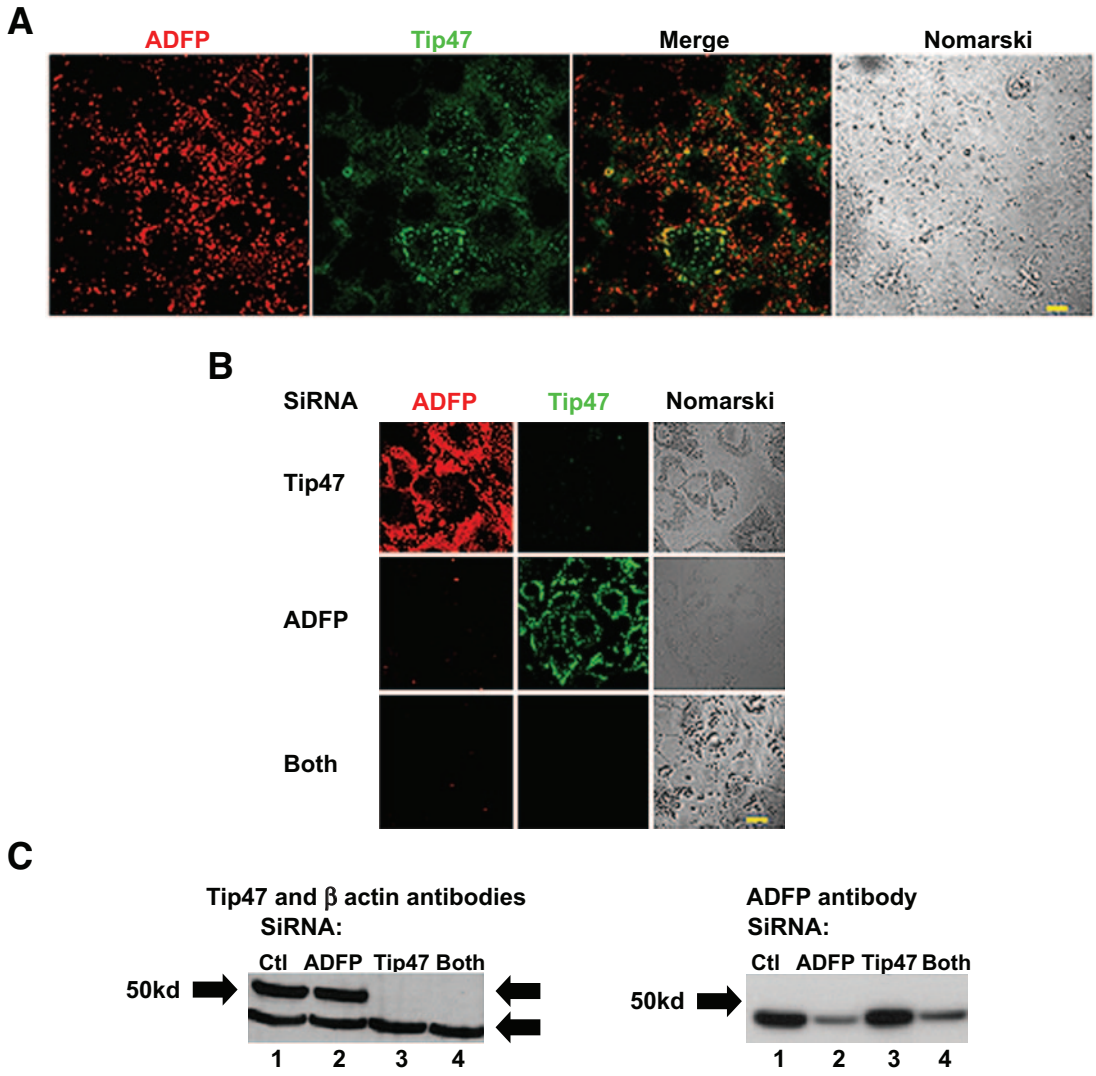

FIG. 1. Identification and downregulation of all PAT proteins (ADFP and Tip47) in AML12 cells. *A*: Cells were incubated with 400 μmol/l oleic acid for 12 h before staining. Cells were costained with a polyclonal goat anti-ADFP antibody and with a rabbit polyclonal anti-Tip47 antibody and, respectively, alexa fluor 488– or 594–conjugated secondary antibodies. Fluorescent and phase images were generated by an LSM 510 confocal laser microscope. Bar represents 50 μm. *B*: Coimmunostaining with ADFP and Tip47 of AML12 cells treated for 4 days with siRNA ADFP, siRNA Tip47, both combined, or control. Cells were treated as above. *C*: Immunoblots of total cellular protein extract from AML12 cells treated with control siRNA (Qiagen) (*lane 1*); siRNA ADFP (*lane 2*); siRNA Tip47 (*lane 3*); or both combined (*lane 4*). Rabbit polyclonal anti-Tip47, anti-ADFP, and anti–β-actin antibodies were used as loading control. (Please see http://dx.doi.org/10.2337/db07-1383 for a high-quality digital representation of this figure.)

recruited from preexisting cytosolic Tip47. Behavior of PAT proteins in control cell homogenates in response to increased exogenous NEFAs is also different (online appendix Fig. S-1); while ADFP increased proportionally to the exogenous lipid, Tip47 was barely affected. Importantly, knockdown of one or more PAT proteins resulted in substantial changes in LD size and number, as observed by bodipy staining (Fig. 2) (online appendix Figs. S-5*A*–*D* and S-7), phase contrast microscopy (online appendix Fig. S-2), or quantify (Fig. 3). Absence of PAT proteins induced a marked increase in LD size and decrease in LD number (28 ± 2.6 vs. 48.09 ± 6.06 for control; $P < 0.05$). When Tip47 was predominant, the LD morphology appeared similar to control treatment cells. When ADFP was predominant, LD number increased (251.7 ± 22.6 vs. 48.09 ± 6.06 for control; $P < 0.01$) but LD size was smaller. Despite changes in LD morphology, TAG content in cellular extracts of oleic acid–loaded cells was unchanged (Fig. 4*B*). However, total TAG decreased in PAT protein–deprived cells when grown without oleic loading. (Fig. 4*A*). This difference prompted examination of PAT protein effects on lipid metabolism.

Metabolic consequences of altered PAT protein profiles

Lipid metabolism. In cells lacking either ADFP or Tip47, no significant alteration in lipolysis was observed (Fig. 5*A*). However, lipolysis significantly increased up to twofold (Fig. 5*A*) (one-way ANOVA; $P < 0.02$) in AML12 cells lacking both proteins. A recent phenotype reported for ATGL-null mice suggests that ATGL is operative in liver (14). Presence of ATGL in AML12 cells was revealed by ATGL-targeted siRNA treatment (online appendix Fig. S-3), which increased LD, as expected from decreased lipolytic activity from loss of ATGL. In cells lacking PAT proteins, ATGL increased at the LD surface (Fig. 5*B*) (online appendix Fig. S-4). Immunoblot analysis revealed an increase in both ATGL and CGI-58 in fat cakes from these cells (Fig. 5*C*). CGI-58 is known to increase ATGL

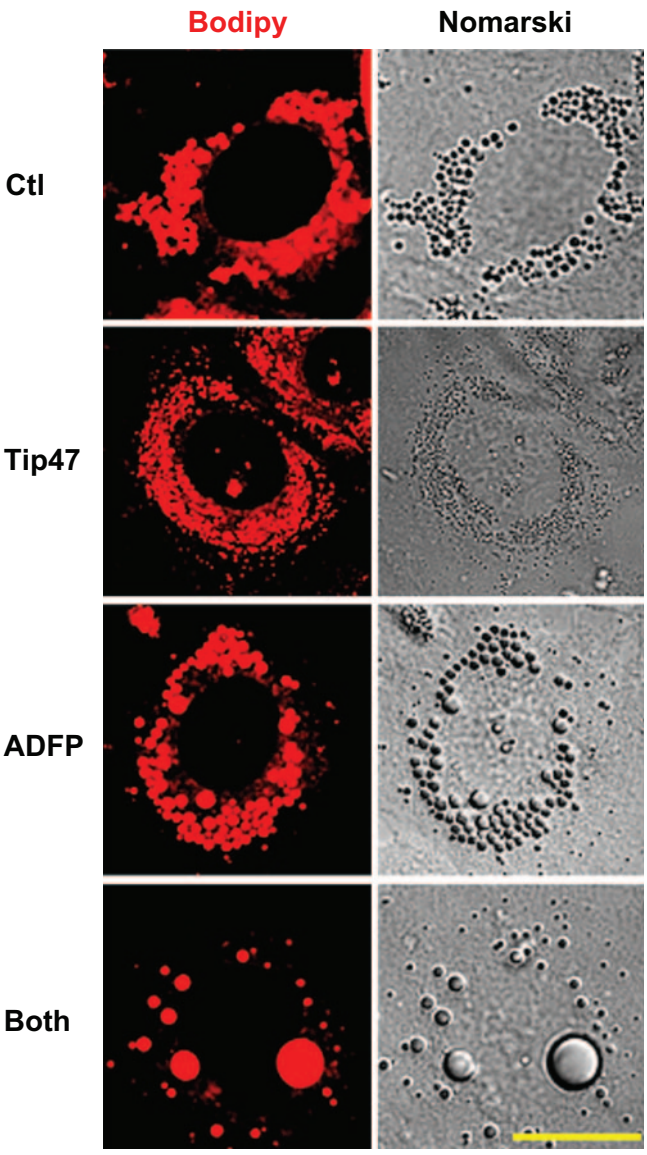

FIG. 2. Morphological differences in AML12 cells following downregulation of PAT proteins. Cells were stained with bodipy fl568, which preferentially stained neutral lipid. Fluorescent and phase images were generated by a LSM 510 confocal laser microscopy. Bar represents 50 μm. (Please see http://dx.doi.org/10.2337/db07-1383 for a high-quality digital representation of this figure.)

activity and to interact with PAT proteins (30). Increase of ATGL at LDs in cells lacking ADFP and Tip47 supports the hypothesis that these proteins limit access of endogenous lipase to the LDs. In contrast, lack of PAT proteins did not affect uptake of ^{3}H exogenous oleic acid and had little influence on the ability of cells to utilize exogenous NEFAs for TAG or phospholipid synthesis (online appendix Fig. S-4). High-performance liquid chromatography analysis did not reveal significant differences in the intracellular content of diacylglycerol (1.45 ± 0.25% [wt/wt] for Ctl vs. 1.4 ± 0.2% [wt/wt]) for cells lacking PAT proteins or ceramide (1.1% in both conditions), but 1.25% (wt/wt) intracellular NEFAs were found in cells lacking PAT proteins, while NEFAs remain undetected in control cells (n = 2 experiments).

Insulin signaling. Because dysregulation of cellular lipid metabolism has been linked to insulin resistance, we measured the effect of PAT siRNA treatment on insulin

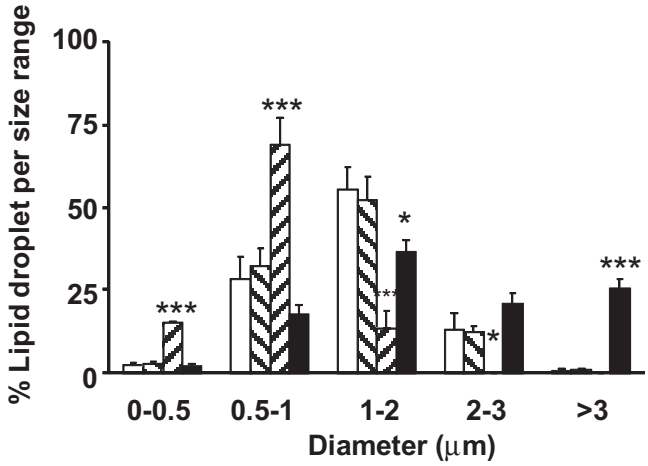

FIG. 3. Composition of the PAT proteins affects the LD size distribution. Number and diameter of LDs were measured following imaging cells treated with siRNA control (Ctl) (Qiagen) (□), both siRNAs Tip47 and ADFP (Both) (■), siRNA ADFP (▨), and siRNA Tip47 (▧). Data are means ± SE from 11 separate experiments for control and ADFP, from three separate experiments for Tip47, and from 27 separate experiments for both. ***P < 0.0001; *P < 0.05 vs. control (t test).

activation of protein kinase B (Akt) in AML12 cells by immunoblot analysis of cellular protein extracts using phosphospecific antibodies. In both control- and siRNA-treated cells, insulin stimulated phosphorylation Akt phos-

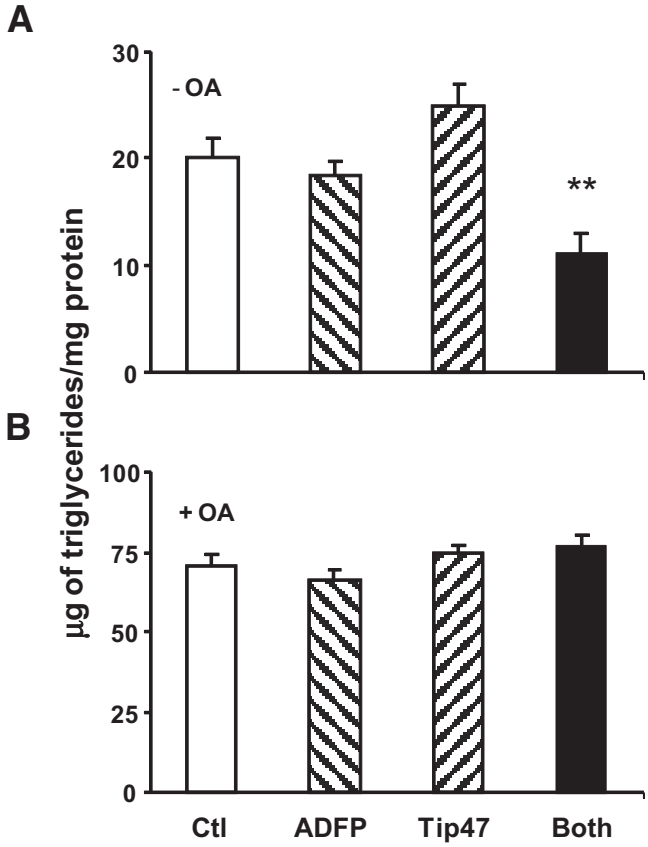

FIG. 4. Absence of exogenous NEFA reveals differences in accumulating lipids in cells lacking ADFP and Tip47. *A*: Triglycerides were measured in cells grown in culture media treated with siRNA control (Qiagen) (□), both siRNAs Tip47 and ADFP (■), siRNA ADFP (▨), and siRNA Tip47 (▧). *B*: Triglycerides were measured in cells grown in culture media supplemented overnight with 400 μmol/l of oleic acid in cells treated as described above. Data are means ± SE from three separate experiments and P < 0.001 (one-way ANOVA) for cells lacking both ADFP and Tip47 grown without exogenous NEFA addition.

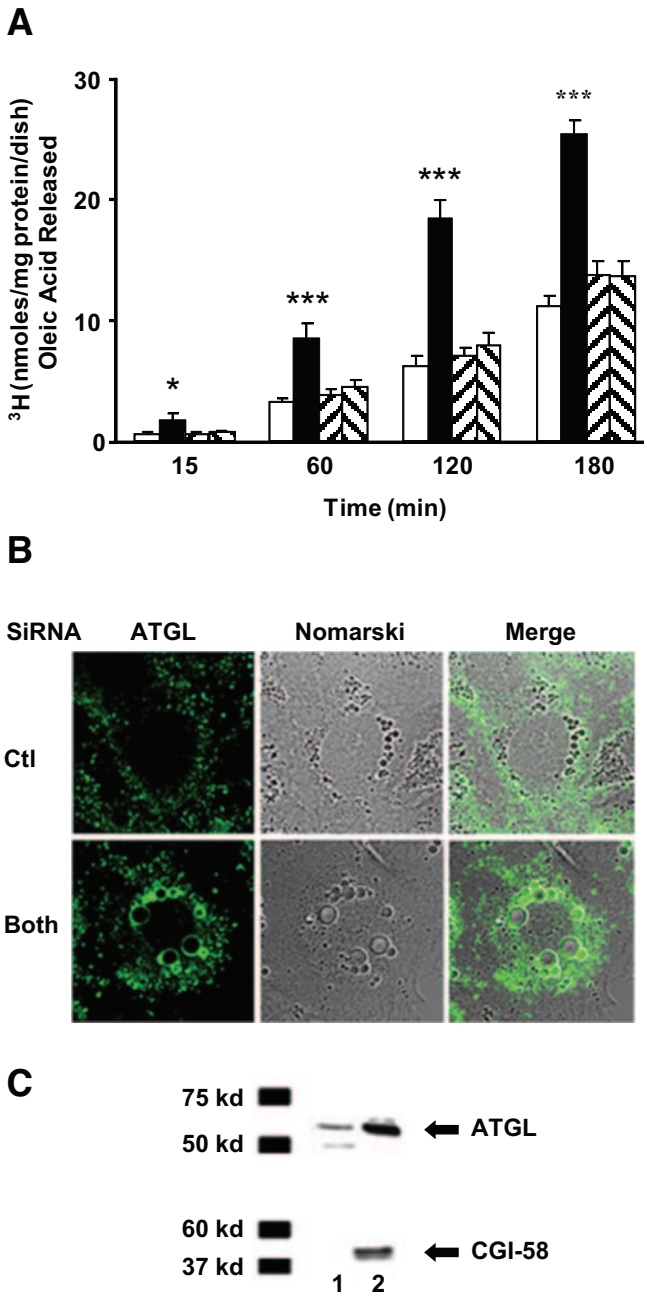

FIG. 5. Increased lipolysis in AML12 cells lacking ADFP and Tip47. *A*: Cells were loaded overnight with two 106 dpm [^{3}H]oleic acid and 400 μmol/l cold oleic acid; the efflux of [^{3}H]oleic acid was tracked over 180 min in the presence of 10 μmol/l triacsin C. Values represent the means ± SE of triplicate determinations of nanomoles released per microgram of protein at time 0, 15, 30, 60, 120, and 180 min. Data are means ± SE from 16 separate experiments for siRNA control and ADFP and Tip47 combined. Data are means ± SE from eight separate experiments for single siRNA transfection with Tip 47 or ADFP. $P < 0.0001$ (one-way ANOVA) for time points 1, 2, and 3 h efflux and $P < 0.002$ (one-way ANOVA) for time point 15 min. *B*: Increase of ATGL and CGI-58 at the LD surface in cells lacking ADFP and Tip47. Immunostaining with ATGL of AML12 cells treated for 4 days with siRNA control or with both combined siRNA ADFP and Tip47. Cells were stained with a polyclonal rabbit ATGL anti-antibody. Alexa fluor 488–conjugated secondary antibodies were used. *C*: Fat cakes resulting from crude fractionation of AML12 cellular extract treated with siRNA: control (Ctl) (*lane 1*) or combined ADFP and Tip47 (*lane 2*). Rabbit polyclonal anti-ATGL and anti–CGI-58 antibodies were used. (Please see http://dx.doi.org/10.2337/db07-1383 for a high-quality digital representation of this figure.)

phorylation at Ser473, an effect previously shown to correlate with the extent of Akt activation in hepatocytes (16). However, absence of PAT proteins resulted in a significant decrease in insulin responsiveness and sensitivity compared with the control (Fig. 6*A* and *B*). Akt phosphorylation was not affected when only one PAT protein was downregulated (results not shown). Effect on Akt phosphorylation was also observed with decreasing concentration of oleic acid in media (online appendix Fig. S-8). To test if increased lipolysis contributed to the observed decrease in insulin responsiveness, cells lacking all PAT proteins were additionally treated with ATGL siRNA. Figure 6*C* shows that the triple inhibition normalized insulin stimulation of Akt to control levels. The total amount of Akt did not differ among the various treatments. Upstream regulation of Akt was also affected by lack of PAT proteins: phosphorylations of PDK-1 (Fig. 7*A*), IRS-1/phosphoinositide 3-kinase activity were decreased in cells lacking PAT proteins (Fig. 7*B*). IRS-1–Ser307 phosphorylation, which promotes general inhibition of IRS-1 signaling (17), was increased in cells lacking PAT proteins (Fig. 7*C*). However, this did not result in a detectable decrease in tyrosine phosphorylation of IRS-1 (results not shown). Downstream targets of Akt, Foxo-1, and GS3-Kα/β were affected (Fig. 7*E* and *F*). Activation of PKC-è was previously shown to be involved in insulin resistance induced by fatty acids (18). Upon insulin stimulation, cells lacking PAT proteins also increased PKC-è protein and phosphorylation in the total cellular membrane fraction (Fig. 6*D*). ERK1/2 phosphorylation was increased in both basal and stimulated conditions in cells lacking PAT proteins (Fig. 7*G*). Overall glucose output was very low in AML112 cells; however, 10^{-8} mol/l insulin was able to suppress glucose output in cells transfected with control siRNA to a greater extent than in cells lacking ADFP and Tip47, confirming a defect in these latter cells in insulin signaling (online appendix Table 1)

In vivo studies. Lack of information on PAT protein and lipase content of liver fat cake in established models of insulin resistance prompted an examination of DIO mice. Liver fat cakes isolated from DIO mice have fourfold-increased lipid content (11.7 ± 2.2% [wt/wt] vs. 3.4 ± 1% [wt/wt]) for ad libitum–fed mice ($P < 0.05$). Importantly, ATGL content also increased (Fig. 8). Despite the large increase in lipids, a matching increase was observed only for LSPD-5, while a significant change in Tip47 was not found and the increase in ADFP appears modest.

DISCUSSION

Using siRNA technology, we were able to develop evidence supporting the role of the PAT proteins in the regulation of ectopic fat deposition and demonstrate the importance of defected LD utilization in the development of cellular insulin resistance. First, the composition of PAT proteins at the LD surface dictates their size and number. Second, the affinity of ADFP may be greater than Tip47 for binding to LDs. Third, the PAT proteins help maintain intracellular NEFA homeostasis by protecting the LDs against lipolysis by decreasing the recruitment of ATGL at the LD surface. Fourth, lack of PAT proteins induces cellular insulin resistance and affects multiple steps in the insulin signaling pathway. Fifth, DIO liver fat cakes differ in their content of PAT proteins and ATGL.

In this study, a loss-of-function approach was developed using siRNA-targeting PAT proteins in a liver cell line

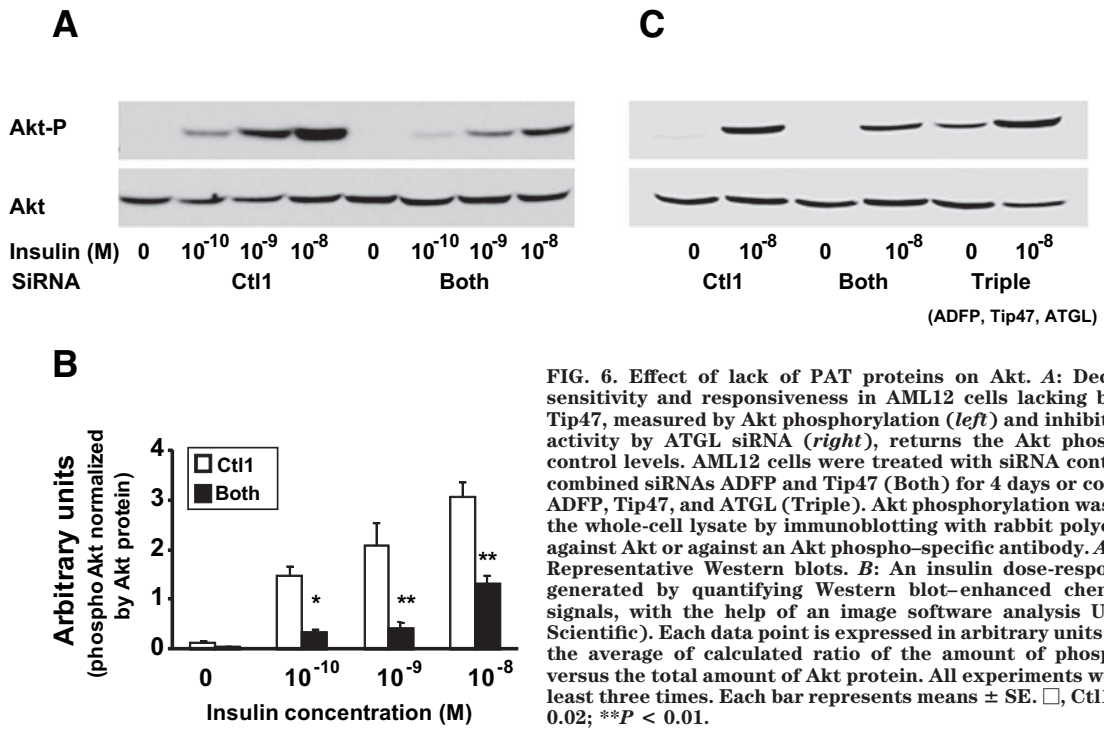

FIG. 6. Effect of lack of PAT proteins on Akt. *A*: Decreased insulin sensitivity and responsiveness in AML12 cells lacking both ADFP and Tip47, measured by Akt phosphorylation (*left*) and inhibition of lipolytic activity by ATGL siRNA (*right*), returns the Akt phosphorylation to control levels. AML12 cells were treated with siRNA control 1 (Ctl1) or combined siRNAs ADFP and Tip47 (Both) for 4 days or combined siRNAs ADFP, Tip47, and ATGL (Triple). Akt phosphorylation was determined in the whole-cell lysate by immunoblotting with rabbit polyclonal antibody against Akt or against an Akt phospho–specific antibody. *A*: *left* and *right*: Representative Western blots. *B*: An insulin dose-response curve was generated by quantifying Western blot–enhanced chemiluminescence signals, with the help of an image software analysis UN-scan-it (Silk Scientific). Each data point is expressed in arbitrary units and represents the average of calculated ratio of the amount of phosphorylated Akt versus the total amount of Akt protein. All experiments were repeated at least three times. Each bar represents means ± SE. □, Ctl1; ■, Both. *P < 0.02; **P < 0.01.

because such a system provides a model for one of the most important tissues where ectopic fat develops. The value of a loss-of-function approach for PAT proteins has been proven with the perilipin-null mice, which exhibit a lean phenotype and enable identification of its regulatory role of lipolysis (19,20). However, the ADFP-null mice exhibit few phenotypic alterations (22), attributed tentatively to a compensatory replacement by Tip47 (12). Further analyses of ADFP-null fibroblast cells treated with siRNA against Tip47 supported the importance of the PAT proteins' role in lipid metabolism (12). AML12 cells are attractive for studies of LDs and insulin signaling (15,23).

Only two PAT proteins, ADFP and Tip47, were found in AML12 cells, predominately ADFP at the liver LD surface (25), whereas Tip47 was observed on some droplets but mainly in the cytosol. This corroborates previous findings that Tip47 and ADFP behave differently in most cells in that Tip47 can be present both in the cytosol and at the LD while ADFP is seen primarily at the LD upon lipid-loaded conditions (25). Inhibition of ADFP expression resulted in increased Tip47 at the LD surface in AML12 cells, similar to our earlier report with cells from ADFP-null mice, suggesting that ADFP has a greater affinity for LDs than Tip47. Thus, when ADFP expression is inhibited, Tip47 moves to the LD surface without major change in LD size and number. However, if Tip47 is repressed, ADFP is then the only PAT protein present and the LD number increases while the sizes decrease. This morphological change may reflect ADFP's greater ability to bind to LDs and greater surfactant function. Finally, absence of both PAT proteins generated fewer but larger LDs. Since PAT proteins have surfactant properties, in their absence LDs probably fuse to minimize surface area contact with the surrounding aqueous cytosol. These studies demonstrate that the PAT protein composition in liver cells is a critical determinant of LD size and number.

Interestingly, varying the LD coat protein did not affect the ability of cells to take up exogenous NEFAs and to esterify it into TAG. Thus, ADFP and Tip47 are not important factors in determining the amount of TAG produced, but they are important factors in determining how it is packaged. However, without PAT proteins, TAG lipolysis increased, demonstrating a function of these two PAT proteins to inhibit LD hydrolysis by endogenous lipase(s). This property is a feature shared for most PAT proteins. Perilipin is known to regulate lipid storage in adipose cells (21,42), and published studies support that ADFP (34), Tip47 (12), and, recently, LSDP-5 (13) protect LD TAG against lipolysis.

Endogenous lipases in liver cells responsible for LD turnover have not yet been catalogued to the same extent as in adipose tissue (26). The phenotype of ATGL-null mice indicates that it may be an important lipase not only in adipose tissue but also in nonadipose tissue. Notably, hepatic fat content was doubled in ATGL-null mice compared with wild-type (14). Interestingly, by imunocytochemistry and immunoblot analysis, we found an ATGL increase at the LD surface when all PAT proteins were absent, confirming a recent report (44) that the lack of ADFP increases ATGL presence in fibroblasts. Furthermore, by downregulating ATGL expression, we could show an active role of ATGL in LD turnover, as judged by increased LDs in cells lacking this lipase. These results led us to hypothesize that ATGL is one of the enzymes participating in LD hydrolysis in liver cells and, importantly, that nonadipose tissue PAT proteins also have a role in inhibiting LD hydrolysis.

A recent finding on ATGL regulation is that this enzyme appears to require CGI-58 for full activity in cytosolic extracts (27). CGI-58 is a protein that when mutated or truncated has been found to be responsible for LD accumulation in most tissues (Chanarin-Dorfman syndrome) (28,29). Most recently, CGI-58 was identified to bind to Perilipin and ADFP (30,31). In our studies, fat cake extract from cells lacking PAT proteins was enriched in CGI-58 protein. This led us to hypothesize that common mechanisms exist among PAT proteins to regulate ATGL access to the LD surface, both in adipose and nonadipose tissues.

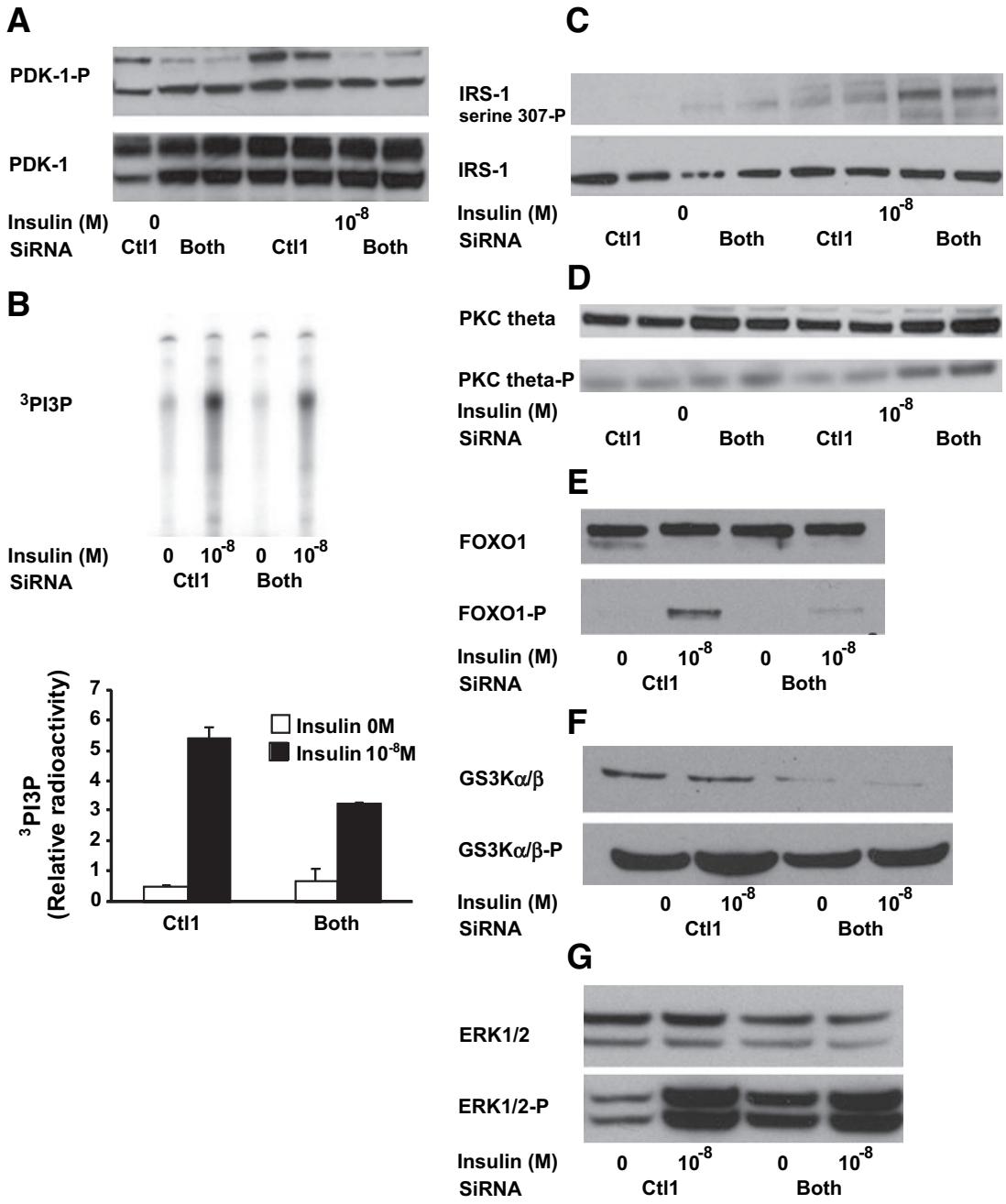

FIG. 7. Insulin signaling steps upstream and downstream from Akt are also perturbed in cells lacking both Tip47 and ADFP. AML12 cells were cultured as above. On the day of the experiment, cells were treated with no or 10^{-8} mol/l insulin for 15 min prior to being scraped. *A*: PDK-1 phosphorylation is decreased in AML12 cells lacking ADFP and Tip47. PDK-1 phosphorylation was determined in the whole-cell lysate by immunoblotting with rabbit polyclonal antibody against PDK-1 or against a PDK-1 phospho-specific antibody. *B*: Cellular extracts were immunoprecipitated with an anti–IRS-1 antibody, and phosphatidylinositol 3-kinase activity was measured. Results are means ± SE arbitrary units. *$P < 0.05$ vs. basal of each group, PIP3, and phosphatidylinositol 3,4,5,-triphosphate. *C*: IRS-1 serine 307 phosphorylation was determined in the whole-cell lysate by immunoblotting with rabbit polyclonal antibody against IRS-1 or against an IRS-1 phospho–specific antibody (Upstate Cell Signaling Solutions). *D*: Activation of PKCθ in AML12 cells lacking both ADFP and Tip47. Activation of PKCθ was determined with phospho-specific antibodies to PKCθ (Thr538). Pellets were obtained by centrifuging the whole-cell lysate at 10,000*g*. The experiment was repeated three times with consistent results. *E*: Activation of Foxo-1 in AML12 cells lacking both ADFP and Tip47. *F*: Activation of GS3α kinase in AML12 cells lacking both ADFP and Tip47. *G*: Activation of ERK1/2 in AML12 cells lacking both ADFP and Tip47.

We found that PAT protein downregulation is sufficient to induce insulin resistance in liver cells. These results led us to conclude that the mechanism underlying the defect in insulin resistance in the absence of PAT proteins is due at least in part to an increase in lipolytic rate and/or uncoupling to NEFA utilization. Absence of PAT proteins at the LD surface facilitates access of endogenous triglyceride lipases such as ATGL to the TAG substrate, releasing NEFAs that in turn affect the signaling cascade at multiple levels. These findings support our working hypothesis that ADFP and Tip47 play important roles in the regulation of ectopic fat, similar to the key role of perilipin in adipose tissue, and that their function can explain at least partially the connection between ectopic fat and development of insulin resistance. If true, then alteration in the composition and/or activity of PAT proteins will result in dysfunc-

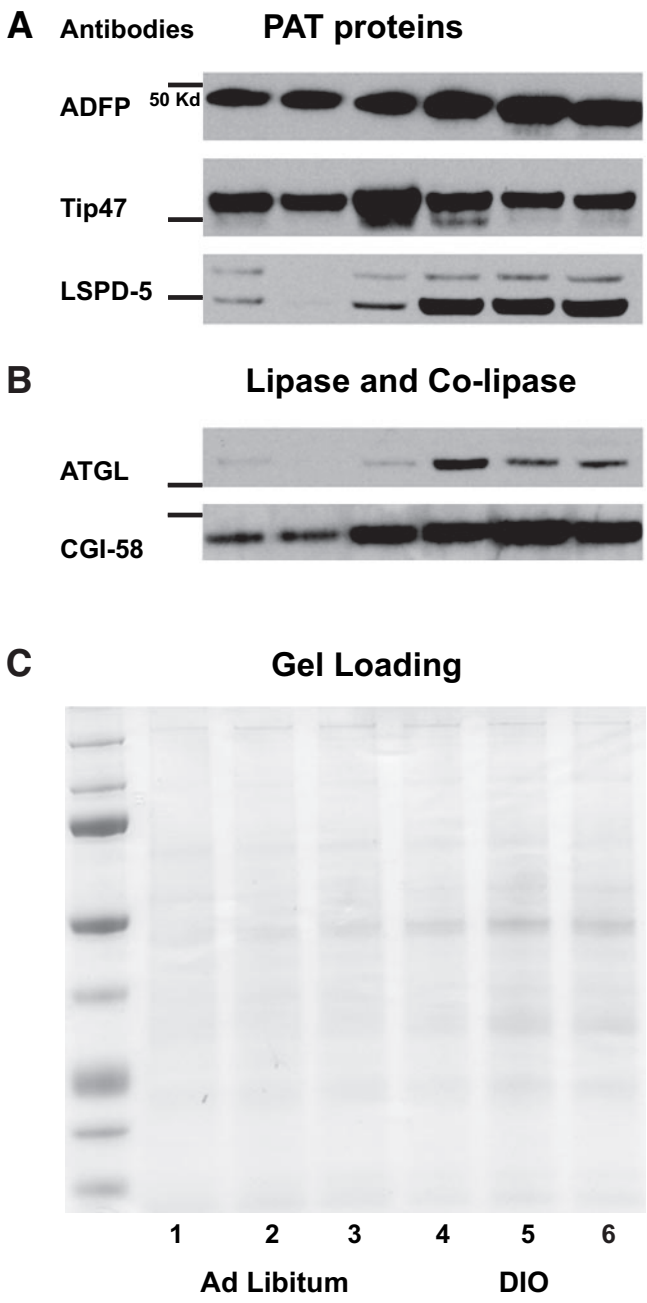

FIG. 8. Content of PAT proteins in DIO mice liver fat cake appears insufficient to protect the LD against the presence of increased ATGL. Fat cakes extracted from three pooled liver tissues from eight mice fed ad libitum or nine DIO mice were loaded in *lanes 1–3* or *lanes 4–6*, respectively. Fat cakes were isolated by ultracentifugation, 10-μl aliquots used for protein determination following cold acetone precipitation overnight, and the protein pellets washed. Equal amounts of total protein were loaded but for ADFP, and 1/20 dilution was performed before loading the samples to avoid overexposed blots.

tional lipolysis triggering a cascade of deleterious events in cellular function. Hence, a strong connection should be visible in nonadipogenic tissues between PAT protein composition, surface protein content, lipolysis, and insulin signaling. However, an in vivo study (45) of ADFP antisense downregulation in liver reported improved insulin sensitivity; no change in VLDL secretion, contrary to cell culture study results (47); and no compensation by Tip47, at least in the whole cellular extract. However, no attempt was reported to assess LPSD-5 presence/activity, while its expression has been shown to correlate with increased β-oxidation and is present in liver (46). Knowing the redundancy with the PAT protein family, LSDP-5 may be responsible for the apparent discrepancy existing between these in vivo results and cell culture (47). The presence of LSDP-5 in liver LDs brings another level of complexity to the regulation of LD utilization. To date, little knowledge exists of LD PAT protein composition in insulin resistance models. We show here that liver LDs from the DIO disease model differ in the ratio of PAT proteins at the LD surface and, importantly, that ATGL is increased at the LD surface. Since ATGL-null mice have increased insulin sensitivity, we hypothesize that defects increasing ATGL access to the lipid surface and/or activity will have the opposite effect (i.e., promote insulin resistance). Thus, we hypothesize that DIO alters liver lipid turnover, contributing to insulin resistance.

It is widely accepted that excessive free fatty acid–induced insulin resistance involves intramyocellular and intrahepatocellular accumulation of TAG, activation of several serine/threonine kinases, reduction in tyrosine phosphorylation of IRS-1/2, and impairment of IRS/phosphoinositide 3-kinase pathway (32) and ERK1/2 pathway (32). Attention has been given in the literature thus far to a failure of mitochondrial oxidative function, but little thought has been given to the failure of the LD compartment to appropriately store the excess NEFAs (34). The results from these studies indicate that defects in LD lipolysis/utilization contribute to loss of ability of nonadipose tissue to maintain NEFA homeostasis and thus are responsible for deleterious consequences observed in the signaling pathway. These defects likely occur in the function/activity of the PAT family LD surface proteins regulating lipolysis. Future research focusing on LD utilization and its regulation will provide us with important clues for understanding regulation of cellular energy homeostasis.

ACKNOWLEDGMENTS

This work was supported by a career development award (1-05-CD-17) from the American Diabetes Association (to C.S.); a grant from the National Institutes of Health (1RO1 DK 075017-01A2 to C.S.); the Geriatric Research, Education and Clinical Center, Baltimore Veterans Affairs Health Care Center; a grant from the Clinical Nutrition Research Unit of Maryland (DK072488 to S.K.F.); and Intramural Research Programs of the National Institute of Diabetes and Digestive and Kidney Diseases and the National Center for Complementary and Alternative Medicine, National Institutes of Health.

We thank Dr. M.C. Woodle for his constant help and support and Dr. A.K. Kimmel for his helpful criticisms.

REFERENCES

1. Meigs JB: Epidemiology of the metabolic syndrome. *Am J Manag Care* 8 (Suppl. 11):S283–S292, 2002
2. Eckel RH, Grundy SM, Zimmet PZ: The metabolic syndrome. *Lancet* 365:1415–428, 2005
3. Shulman GI: cellular mechanisms of insulin resistance. *J Clin Invest* 106:171–176, 2000
4. Gavrilova O, Haluzik M, Matsusue K, Cutson JJ, Johnson L, Dietz KR, Nicole CJ, Vinson C, Gonzalez FJ, Reitman ML: Liver peroxisome proliferator-activated receptor gamma contributes to hepatic steatosis, triglyceride clearance, and regulation of body fat mass. *J Biol Chem* 278:34268–34276, 2003
5. Prentki M, Vischer S, Glennon MC, Regazzi R, Deeney JT, Corkey BE: Malonyl-CoA and long chain acyl-CoA esters as metabolic coupling factors in nutrient-induced insulin secretion. *J Biol Chem* 267:5802–5810, 1992
6. Chiu HC, Kovacs A, Ford DA, Hsu FF, Garcia R, Herrero P, Saffitz JE,

Schaffer JE: A novel mouse model of lipotoxic cardiomyopathy. *J Clin Invest* 107:813–822, 2000
7. Tarnopolsky MA, Rennie CD, Robertshaw HA, Fedak-Tarnopolsky SN, Devries MC, Hamadeh MJ: Influence of endurance exercise training and sex on intramyocellular lipid and mitochondrial ultrastructure, substrate use, and mitochondrial enzyme activity. *Am J Physiol Regul Integr Comp Physiol* 292:R1271–R1278, 2007
8. Murphy DJ, Vance J: Mechanisms of lipid-body formation. *Trends Biochem Sci* 3:109–115, 1999
9. Listenberger LL, Han X, Lewis SE, Cases S, Farese RV Jr, Ory DS, Schaffer JE: Triglyceride accumulation protects against fatty acid-induced lipotoxicity. *Curr Opin Lipidol* 3:281–287, 2003
10. Miura S, Gan JW, Brzostowski J, Parisi MJ, Schultz CJ, Londos C, Oliver B, Kimmel AR: Functional conservation for lipid storage droplet association among Perilipin, ADRP, and TIP47 (PAT)-related proteins in mammals, Drosophila, and Dictyostelium. *J Biol Chem* 277:32253–32257, 2002
11. Lu X, Gruia-Gray J, Copeland NG, Gilbert DJ, Jenkins NA, Londos C, Kimmel AR: The murine perilipin gene: the lipid droplet-associated perilipins derive from tissue-specific, mRNA splice variants and define a gene family of ancient origin. *Mamm Genome* 9:741–749, 2001
12. Sztalryd C, Bell M, Lu X, Mertz P, Hickenbottom S, Chang BH, Chan L, Kimmel AR, Londos L: Functional compensation for adipose differentiation-related protein (ADFP) by Tip47 in an ADFP null embryonic cell line. *J Biol Chem* 281:34341–34348, 2006
13. Dalen KT, Dahl T, Holter E, Amtsen B, Londos C, Sztalryd C, Nebb HI: LSDP5 is a PAT protein specifically expressed in fatty acid oxidizing tissues. *Biochim Biophys Acta* 17712:210–227, 2007
14. Haemmerle G, Lass A, Zimmermann R, Gorkiewicz G, Meyer C, Rozman J, Heldmaier G, Maier C, Theussl S, Eder D, Kratky EF, Wagner M, Klingenspor G, Hoefler G, Zechner R: Defective lipolysis and altered energy metabolism in mice lacking adipose triglyceride lipase. *Science* 312:734–737, 2006
15. Butler M, McKay RA, Popoff IJ, Gaarde WA, Witchell D, Murray SF, Dean NM, Bhanot S, Monia BP: Specific inhibition of PTEN expression reverses hyperglycemia in diabetic mice. *Diabetes* 51:1028–1034, 2002
16. Kandel ES, Hay N: The regulation and activities of the multifunctional serine/threonine kinase Akt/PKB. *Exp Cell Res* 253:210–229, 1999
17. Aguirre V, Werner ED, Giraud J, Lee YH, Shoelson SE, White MF: Phosphorylation of Ser307 in insulin receptor substrate-1 blocks interactions with the insulin receptor and inhibits insulin action. *J Biol Chem* 2:1531–1537, 2002
18. Kim JK, Fillmore JJ, Sunshine MJ, Albrecht B, Higashimori T, Kim DW, Liu ZX, Soos TJ, Cline GW, O'Brien WR, Littman DR, Shulman GI: PKC-ϑ knockout mice are protected from fat-induced insulin resistance. *J Clin Inv* 114:823–827, 2004
19. Martinez-Botas J, Anderson JB, Tessier D, Lapillonne A, Chang BH, Quast MJ, Gorenstein D, Chen KH, Chan L: Absence of perilipin results in leanness and reverses obesity in Lepr(db/db) mice. *Nat Genet* 4:474–479, 2000
20. Tansey JT, Sztalryd C, Gruia-Gray J, Roush DL, Zee JV, Gavrilova O, Reitman ML, Deng CX, Li C, Kimmel AR, Londos C: Perilipin ablation results in a lean mouse with aberrant adipocyte lipolysis, enhanced leptin production, and resistance to diet-induced obesity. *Proc Natl Acad Sci U S A* 98:6494–6499, 2001
21. Sztalryd C, Xu G, Dorward H, Tansey JT, Contreras JA, Kimmel AR, Londos C: Perilipin A is essential for the translocation of hormone-sensitive lipase during lipolytic activation. *J Cell Biol* 161:1093–1103, 2003
22. Chang BH, Li L, Paul A, Taniguchi S, Nannegari V, Heird WC, Chan L: Protection against fatty liver but normal adipogenesis in mice lacking adipose differentiation-related protein. *Mol Cell Biol* 26:1063–1076, 2006
23. Schadinger SE, Bucher NL, Schreiber BM, Farmer SR: PPARγ2 regulates lipogenesis and lipid accumulation in steatotic hepatocytes. *Am J Physiol Endocrinol Metab* 288:E1195–E1205, 2005
24. Dalen KT, Ulven SM, Amtsen BM, Solaas K, Nebb HI: PPARα activators and fasting induce the expression of adipose differentiation-related protein in liver. *J Lipid Res* 47:931–943, 2006
25. Wolins NE, Rubin B, Brasaemle DL: TIP47 associates with lipid droplets. *J Biol Chem* 276:5101–108, 2001
26. Birner-Gruenberger R, Susani-Etzerodt H, Waldhuber M, Riesenhuber G, Schmidinger H, Rechberger G, Kooroser M, Strauss JG, Lass A, Zimmermann R, Haemmerle G, Zechner R, Hermetter A: The lipolytic proteome of mouse adipose tissue. *Mol Cell Proteonomics* 11:1710–1717, 2005
27. Lass A, Zimmermann R, Haemmerle G, Riederer M, Schoiswohl G, Schweiger M, Kienesberger P, Strauss J, Gorkiewicz G, Zechner R: Adipose triglyceride lipase-mediated lipolysis of cellular fat stores is activated by CGI-58 and defective in Chanarin-Dorfman Syndrome. *Cell Metab* 3:309–319, 2006
28. Lefèvre C, Jobard F, Caux F, Bouadjar B, Karaduman A, Heilig R, Lakhdar H, Wollenberg A, Verret J-L, Weissenbach J, Özgüc M, Lathrop M, Prud'homme J-F, Fischer J: Mutations in CGI-58, the gene encoding a new protein of the esterase/lipase/thioesterase subfamily, in Chanarin-Dorfman syndrome. *Am J Hum Genet* 69:1002–1012, 2001
29. Akiyama M, Sawamura D, Nomura Y, Sugawara M, Shimizu H: Truncation of CGI-58 protein causes malformation of lamellar granules resulting in ichthyosis in Dorfman-Chanarin syndrome. *J Invest Dermatol* 125:1029–1034, 2003
30. Yamaguchi T, Omatsu N, Matsushita S, Osumi T: CGI-58 interacts with perilipin and is localized to lipid droplets: possible involvement of CGI-58 mislocalization in Chanarin-Dorfman syndrome. *J Biol Chem* 279:30490–30497, 2004
31. Subramanian V, Rothenberg A, Gomez C, Cohen AW, Garcia A, Bhattacharyya S, Shapiro L, Dolios G, Wang R, Lisanti MP, Brasaemle DL: Perilipin A mediates the reversible binding of CGI-58 to lipid droplets in 3T3–L1 adipocytes. *J Biol Chem* 279:42062–42071, 2004
32. Boden G: Fatty acid-induced inflammation and insulin resistance in skeletal muscle and liver. *Curr Diab Rep* 6:177–181, 2006
33. Schrauwen P, Hesselink MK: Oxidative capacity, lipotoxicity, and mitochondrial damage in type 2 diabetes. *Diabetes* 53:1412–1417, 2004
34. Xu G, Sztalryd C, Lu X, Tansey J, Gan J, Dorward H, Kimmel AR, Londos C: Post-translational regulation of adipose differentiation-related protein by the ubiquitin/proteasome pathway. *J Biol Chem* 280:42841–42847, 2005
35. Kershaw EE, Hamm JK, Verhagen LA, Peroni O, Katic M, Flier JS: Adipose triglyceride lipase: function, regulation by insulin, and comparison with adiponutrin. *Diabetes* 55:148–157, 2006
36. Gao Z, Zhang X, Zuberi A, Hwang D, Quon MJ, Lefevre M, Ye J: Inhibition of insulin sensitivity by free fatty acids requires activation of multiple serine kinases in 3T3–L1 adipocytes. *J Mol Endocrinol* 18:2024–2034, 2004
37. Sztalryd C, Levacher C, Picon L: Acceleration by triiodothyronine of adipose conversion of rat preadipocytes from two adipose localizations. *Cell Mol Biol* 35:81–88, 1989
38. Igal RA, Wang P, Coleman RA: Triacsin C blocks de novo synthesis of glycerolipids and cholesterol esters but not recycling of fatty acid into phospholipid: evidence for functionally separate pools of acyl-CoA. *Biochem J* 324:529–534, 1997
39. Tansey JT, Huml AM, Vogt R, Davis KE, Jones JM, Fraser KA, Brasaemle DL, Kimmel AR, Londos C: Functional studies on native and mutated forms of perilipins: a role in protein kinase A-mediated lipolysis of triacylglycerols. *J Biol Chem* 278:8401–8406, 2003
40. Dole VP: Fractionation of plasma nonesterified fatty acids. *Proc Soc Exp Biol Med* 93:532–533, 1956
41. Bligh EG, Dyer WJ: A rapid method of total lipid extraction and purification. *Can J Biochem Physiol* 37:911–917, 1959
42. Brasaemle DL, Rubin B, Harten IA, Gruia-Gray J, Kimmel AR, Londos C: Perilipin A increases triacylglycerol storage by decreasing the rate of triacylglycerol hydrolysis. *J Biol Chem* 275:38486–38493, 2000
43. Stith BJ, Hall J, Ayres P, Waggoner L, Moore JD, Shaw WA: Quantification of major clases of Xenopus phospholipids by high performance liquid chromatography with evaporative light scattering detection. *J Lipid Res* 41;1448–1454, 2000
44. Listenberger LL, Ostermeyer-Fay AG, Goldberg EB, Brown WJ, Brown DA: Adipocyte differentiation-related protein reduces the lipid droplet association of adipose triglyceride lipase and slows triacylglycerol turnover. *J Lipid Res* 48:2751–2761, 2007
45. Imai Y, Varela GM, Jackson MB, Graham MJ, Crooke RM, Ahima RS: Reduction of hepatosteatosis and lipid levels by an adipose differentiation-related protein antisense oligonucleotide. *Gastroenterology* 132:1947–1954, 2007
46. Wolins NE, Quaynor BK, Skinner JR, Tzekov A, Croce MA, Gropler MC, Varma V, Yao-Borengasser A, Rasouli N, Kern PA, Finck BN, Bickel PE: OXPAT/PAT-1 is a PPAR-induced lipid droplet protein that promotes fatty acid utilization. *Diabetes* 12:3418–3428, 2006
47. Magnusson B, Asp L, Boström P, Ruiz M, Stillemark-Billton P, Lindén D, Borén J, Olofsson SO: Adipocyte differentiation-related protein promotes fatty acid storage in cytosolic triglycerides and inhibits secretion of very low-density lipoproteins. *Arterioscler Thromb Vasc Biol* 7:1566–1571, 2006
48. Berasi SP, Huard C, Dongmei L, Shih HH, Sun Y, Zhong W, Paulsen JE, Brown EL, Gimeno RE, Martinez RV: Inhibition og gluconeogenesis through transcriptional activation of EGR1 and DUSP4 by AMP-activated kinase. *J Biol Chem* 281:27167–27177, 2006